

# Copper clusters built on bulky amidinate ligands: spin delocalization *via* superexchange rather than direct metal–metal bonding†

Xuan Jiang, John C. Bollinger, Mu-Hyun Baik\* and Dongwhan Lee\*

Received (in Cambridge, UK) 6th August 2004, Accepted 17th November 2004

First published as an Advance Article on the web 10th January 2005

DOI: 10.1039/b412152j

Entry into a new class of tetra- and dicopper clusters was assisted by a fine steric tuning of bulky amidinate ligands that provide spin-delocalizing superexchange pathways in class III mixed-valence clusters, the properties of which are best understood without invoking metal–metal bonding.

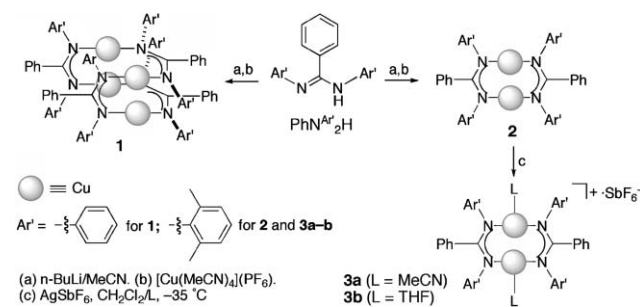
Valence-delocalized transition metal clusters often participate in electron transfer (ET) processes in living systems.<sup>1</sup> The dinuclear Cu<sub>A</sub> sites in cytochrome *c* oxidase and nitrous oxide reductase represent one such example, in which a rapid switching between Cu<sub>2</sub>(I,I) and Cu<sub>2</sub>(I,II) states accompanies electron shuttling.<sup>2</sup> Synthetic analogues of these dicopper sites have previously been achieved using multiaza chelating ligands,<sup>3</sup> conformationally rigid or sterically demanding carboxylate ligands,<sup>4</sup> or a thioether-appended amido ligand.<sup>5</sup> The relatively short Cu⋯Cu distances determined for both biological (~2.5 Å) and synthetic (2.36–2.42 Å) systems have often been invoked to rationalize spin delocalization *via* direct Cu–Cu bonding.<sup>2</sup> It remains to be established whether such a direct metal–metal interaction is a prerequisite for spin delocalization in copper dimers that lack single-atom bridging ligands. In this communication, we disclose a synthetic strategy that allowed access to discrete tetra- and dicopper amidinate complexes. A copper(I) dimer having two-coordinate metal centers was obtained, which undergoes two consecutive one-electron redox processes in solution. One-electron chemical oxidation of this compound afforded class III dicopper(I,II) complexes. Despite a short Cu⋯Cu distance, spin delocalization in this dicopper(I,II) core is dominated by superexchange through  $\mu$ -1,3 bridging ligands.

Anion metathesis of a simple copper(I) salt with *N,N*-disubstituted amidinates in MeCN cleanly afforded neutral compounds that precipitated from the reaction mixture in isolated yields exceeding 85% (Scheme 1). Highly simplified <sup>1</sup>H- and <sup>13</sup>C-NMR resonances displayed by these products indicated a symmetric ligand environment. The solid-state structure of the tetracopper(I) complex [Cu<sub>4</sub>( $\mu$ -N<sup>Ph</sup><sub>2</sub>CPh)<sub>4</sub>] (**1**) was determined by X-ray crystallography on yellow crystals obtained by vapor diffusion of pentanes into a saturated CH<sub>2</sub>Cl<sub>2</sub> solution of this material.† As shown in Fig. 1, the core structure **1** features a pseudo-rhombic Cu<sub>4</sub> center, in which Cu⋯Cu distances of 2.5674(6)–2.6419(7) Å are spanned by  $\mu$ -1,3-bridging amidinates disposed alternately above and below the Cu<sub>4</sub> plane. Topologically

related Cu<sub>4</sub> cores have previously been obtained using carboxylate (RCO<sub>2</sub><sup>−</sup>, R = C<sub>6</sub>H<sub>5</sub>; CF<sub>3</sub>)<sup>6</sup> or triazinate (NN<sup>R</sup><sub>2</sub><sup>−</sup>, R = CH<sub>3</sub>)<sup>7</sup> ligands, which are isoelectronic with amidinate. Despite the extensive use of amidinate ligands to support essentially every metal ion across the periodic table,<sup>8</sup> tetracopper clusters of this robust bidentate ligand were previously unknown.

In **1**, *ortho* hydrogen atoms on the *N*-phenyl groups are pointing toward the phenyl rings of the neighboring ligands. Installing alkyl groups on the 2,6-positions of the phenyl ring was thus expected to maximize interligand steric crowding and assist the assembly of lower nuclearity copper(I) clusters. A bulkier amidinate ligand *N,N'*-bis(2,6-dimethylphenyl)benzamidinate was thus deployed to prepare a dicopper(I) complex [Cu<sub>2</sub>( $\mu$ -N<sup>Me</sup><sub>2</sub>Ph<sub>2</sub>CPh)<sub>2</sub>] (**2**) (Fig. 1).‡ The relatively short Cu⋯Cu separation of 2.4571(2) Å in **2** is comparable to those (2.414(1)–2.497(2) Å) obtained for other rare examples of bis(amidinate)dicopper(I) complexes.<sup>9</sup>

In CH<sub>2</sub>Cl<sub>2</sub>, **2** undergoes two consecutive redox processes as determined by cyclic voltammetry and square wave voltammetry (Fig. S1).†<sup>10</sup> The two quasi-reversible redox waves centered



Scheme 1 Synthesis of copper amidinate complexes.

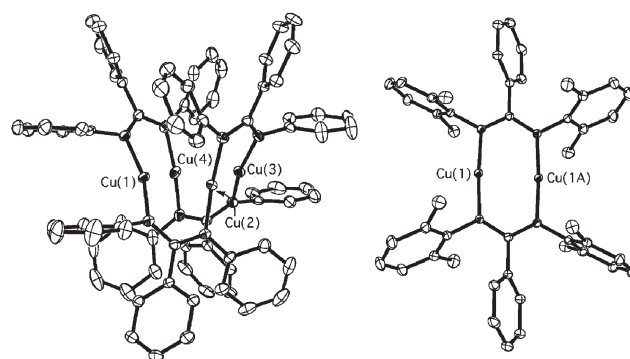


Fig. 1 ORTEP diagrams of **1** (left) and **2** (right) with thermal ellipsoids at 50% probability.

† Electronic supplementary information (ESI) available: details of the synthetic procedures, crystallographic data, and DFT calculations. See <http://www.rsc.org/suppdata/cc/b412152j/>  
\*mbaik@indiana.edu (Mu-Hyun Baik)  
dongwhan@indiana.edu (Dongwhan Lee)

at 0.31 and 0.79 V were assigned to  $\text{Cu}_2(\text{I,I})/\text{Cu}_2(\text{I,II})$  and  $\text{Cu}_2(\text{I,II})/\text{Cu}_2(\text{II,II})$  redox couples, respectively. High-level DFT calculations coupled to a continuum solvation model<sup>11</sup> support this assignment. Our calculations place the two oxidation potentials at 0.461 and 0.986 V, thus overestimating both metal-based redox potentials by 151 and 196 mV, respectively.<sup>§</sup> The computed potential difference between the two redox events of 525 mV, however, is in excellent agreement with the experimental value of 480 mV.<sup>¶</sup> A large comproportionation constant of  $K_{\text{com}} = 1.3 \times 10^8$  for the equilibrium between  $\text{Cu(I)Cu(I)} + \text{Cu(II)Cu(II)}$  and  $\text{Cu(I)Cu(II)}$  species<sup>12</sup> indicates a significant thermodynamic stability of the electrochemically generated  $\text{Cu}_2(\text{I,II})$  complex, prompting us to explore synthetic routes to access them.

Initial attempts to oxidize **2** using various Ag(I) reagents did not result in any isolable products. A dark purple–blue species generated in  $\text{CH}_2\text{Cl}_2$  rapidly decayed to yellow–brown product(s), and insoluble materials deposited over time. The stability of this putative  $\text{Cu}_2(\text{I,II})$  species, however, could be enhanced by conducting the reaction in the presence of coordinating solvents such as MeCN or THF at low temperatures (Scheme 1). Analytically pure, purple–blue ( $\lambda_{\text{max}} \sim 680 \text{ nm}$ ;  $\epsilon > 2000 \text{ M}^{-1} \text{ cm}^{-1}$  per dimer in  $\text{CH}_2\text{Cl}_2$ ) crystals of **3a** (73% isolated yield) and **3b** (49% isolated yield) were obtained at  $-35 \text{ }^\circ\text{C}$  and characterized by X-ray crystallography.<sup>‡</sup> As shown in Fig. 2, the **3a** cation reveals two metal centers related by crystallographic inversion symmetry, implicating the valence-delocalized nature of the dicopper(I,II) core. A short  $\text{Cu}\cdots\text{Cu}$  separation of 2.4547(13) Å in **3a** is spanned by two  $\mu$ -1,3 amidinate ligands and the remaining coordination site on each metal center is occupied by an MeCN ligand. An analogous THF complex **3b** has comparable  $\text{Cu}\cdots\text{Cu}$  distances of 2.4423(12) and 2.3974(11) Å, as determined for the two independent molecules in the asymmetric unit (Fig. S2). Cyclic voltammetry of **3a** displays a quasi-reversible redox wave centered at  $E_{1/2}(\text{Cu}_2(\text{I,II})/\text{Cu}_2(\text{I,I})) = 0.29 \text{ V}$ .

The valence-delocalized nature of the dicopper(I,II) center was further confirmed by EPR spectroscopic studies. The seven-line splitting patterns observed at 77 K for a frozen solution sample of **3a** (Fig. 3) is characteristic of a spin interacting with two copper ions ( $I = 3/2$ ). This rhombic signal retains its structure at 4.5 K, at which point features arising from superhyperfine coupling to the nitrogen nuclei become more discernible (Fig. S3). DFT

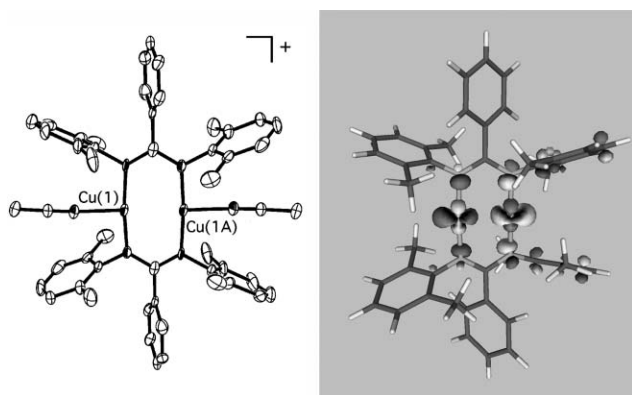


**Fig. 2** ORTEP diagram of **3a** cation with thermal ellipsoids at 50% probability (left) and isosurface plot (0.05 au) of the redox-active MO (the  $\beta$ -LUMO) of  $2^+$  (right).

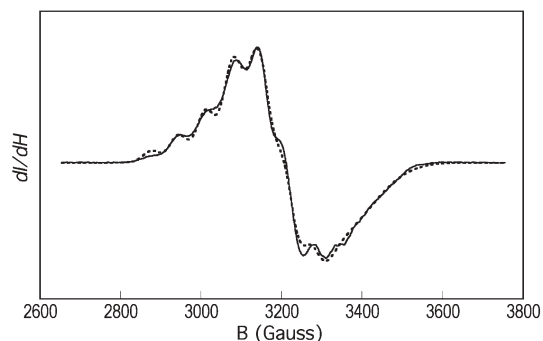


**Fig. 3** X-band EPR spectra (solid lines) of a frozen  $\text{CH}_2\text{Cl}_2$ -toluene (1 : 1, v/v) sample of **3a** measured at 77 K. Simulations (dashed lines) are calculated for  $g_x = 2.022$ ,  $g_y = 2.132$ ,  $g_z = 2.199$ ,  $A_x = 19.4 \text{ G}$ ,  $A_y = 20.9 \text{ G}$ ,  $A_z = 73.7 \text{ G}$ .

calculations are also consistent with the valence-delocalized nature of  $2^+$ , the one-electron oxidation product of **2**. Mulliken spin populations of 0.23 and 0.22 at each of the copper centers in  $2^+$  (Fig. 4) indicate that roughly half of the “extra” electron is distributed equally among the two copper centers whereas the ligand environment absorbs the other half of the spin.<sup>†</sup> Interestingly, almost 30% of the unpaired spin is delocalized over the  $\pi$ -space of the *N*-aryl groups, whereas the four nitrogen atoms accommodate a total of approximately 20% of the unpaired electron. Remarkably, the amidinate carbon atoms and the appended phenyl groups play no role in the spin dissipation process.

Electronically, the two  $\text{Cu(I)-}d^{10}$  centers in the neutral dimer give rise to 10 metal-dominated frontier orbitals that are all filled, thus disqualifying any M–M bonding interaction. The removal of electrons from the high lying MO that is M–M antibonding allows in principle for the formation of a single bond. However, a crucial requirement for oxidation having such impact is that there is

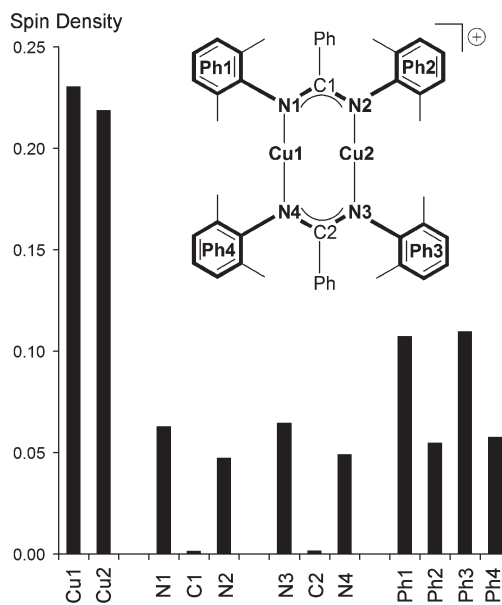


**Fig. 4** Mulliken spin density distribution in  $2^+$ . Regions of the molecule that participate notably in delocalizing the unpaired electron are highlighted in bold.

sufficient overlap of metal d-orbitals along the M–M vector. Fig. 2 shows the redox-active MO, the  $\beta$ -LUMO of  $\mathbf{2}^+$ . It is mainly composed of the Cu  $d_{z^2}$  orbital with some mixing of the  $d_{x^2-y^2}$  orbital, where the z-axis is aligned with the Cu–Cu vector. This MO is best characterized as non-bonding or slightly anti-bonding with respect to both the Cu $\cdots$ Cu centers and along the Cu–N bonds. As a consequence, the first oxidation leads to only an insignificant decrease of the Cu–Cu distance by 0.081 Å and a similarly small average contraction of the Cu–N bonds by 0.031 Å. The non-bonding nature of the redox active MO was further confirmed by the Mayer bond-order analysis.<sup>13</sup> Upon removal of one electron from  $\mathbf{2}$ , the Cu–Cu bond order increases by a negligibly small amount of 0.05 from 0.22 to 0.27, whereas the Cu–N bond orders of 0.50 each remain constant.<sup>14</sup> The bond order invariance is maintained for the removal of the second electron giving a formal Cu–Cu bond order of 0.25 for  $\mathbf{2}^{2+}$ . We note that the removal of the second electron leads to a formal decrease of the Cu–Cu bond order by 0.02, highlighting that bond order changes of this magnitude are physically meaningless and should be interpreted as invariant. The negligible structural change upon metal oxidation promises low inner-sphere energy barriers for ET, an important requirement for future technical exploitations of this redox system.

In summary, through the steric modification of the modular  $\text{ArCN}^{\text{Ar}'}_2^-$  platform, we devised unique synthetic strategies to access tetra- and dicopper clusters from a homologous ligand set. The latter compound undergoes one-electron oxidation to afford well-characterized class III dicopper(I,II) complexes, in which spin-delocalization is mediated by superexchange rather than direct metal–metal bonding. We thank the National Science Foundation (0116050 to Indiana University) and the Indiana University for funding.

**Xuan Jiang, John C. Bollinger, Mu-Hyun Baik\* and Dongwhan Lee\***  
*Department of Chemistry and School of Informatics, Indiana University, Bloomington, IN 47405, USA. E-mail: mbaik@indiana.edu; dongwhan@indiana.edu; Fax: 812 855 8300; Tel: 812 855 9364*

## Notes and references

† *Crystal data.*  $\mathbf{1}\cdot 0.5\text{CH}_2\text{Cl}_2\cdot 0.5\text{C}_5\text{H}_{12}$ :  $\text{C}_{79}\text{H}_{71}\text{ClCu}_4\text{N}_4$ ,  $M = 1366.11$ , triclinic,  $a = 13.666(3)$ ,  $b = 14.295(2)$ ,  $c = 19.401(5)$  Å,  $\alpha = 83.271(12)$ ,  $\beta = 74.874(14)$ ,  $\gamma = 74.361(12)^\circ$ ,  $V = 3518.8(14)$  Å<sup>3</sup>,  $T = 112(2)$  K, space group  $P\bar{1}$ ,  $Z = 1$ ,  $\lambda(\text{Mo-K}\alpha) = 0.71073$  Å, 97467 reflections, 20526 unique ( $R_{\text{int}} = 0.0595$ ),  $R_1 = 0.0437$  for  $I > 2\sigma(I)$ ,  $wR_2 = 0.1172$ .  $\mathbf{2}$ :  $\text{C}_{46}\text{H}_{46}\text{Cu}_2\text{N}_4$ ,  $M = 781.95$ , monoclinic,  $a = 10.9223(8)$ ,  $b = 14.8184(11)$ ,  $c = 11.8480(9)$  Å,  $\beta = 91.315(2)^\circ$ ,  $V = 1917.1(2)$  Å<sup>3</sup>,  $T = 119(2)$  K, space group  $P2_1/n$ ,  $Z = 2$ ,  $\lambda(\text{Mo-K}\alpha) = 0.71073$  Å, 75170 reflections, 11896 unique ( $R_{\text{int}} = 0.0341$ ),  $R_1 = 0.0269$  for  $I > 2\sigma(I)$ ,  $wR_2 = 0.0737$ .  $\mathbf{3a}\cdot \text{C}_2\text{H}_4\text{Cl}_2$ :  $\text{C}_{52}\text{H}_{56}\text{Cl}_2\text{Cu}_2\text{F}_6\text{N}_6\text{Sb}$ ,  $M = 1198.81$ , monoclinic,  $a = 22.385(4)$ ,  $b = 10.4127(18)$ ,  $c = 22.665(4)$  Å,  $\beta = 103.516(4)^\circ$ ,  $V = 5136.6(16)$  Å<sup>3</sup>,  $T = 115(2)$  K, space group  $I2/a$ ,  $Z = 4$ ,  $\lambda(\text{Mo-K}\alpha) = 0.71073$  Å, 29600

reflections, 8469 unique ( $R_{\text{int}} = 0.0939$ ),  $R_1 = 0.0448$  for  $I > 2\sigma(I)$ ,  $wR_2 = 0.0954$ .  $\mathbf{3b}\cdot \text{CH}_2\text{Cl}_2$ :  $\text{C}_{56}\text{H}_{66}\text{Cl}_2\text{Cu}_2\text{F}_6\text{N}_4\text{O}_2\text{Sb}$ ,  $M = 1260.91$ , triclinic,  $a = 12.562(3)$ ,  $b = 21.015(4)$ ,  $c = 21.138(5)$  Å,  $\alpha = 90.899(6)$ ,  $\beta = 104.009(8)$ ,  $\gamma = 91.598(7)^\circ$ ,  $V = 5411(2)$  Å<sup>3</sup>,  $T = 123(2)$  K, space group  $P\bar{1}$ ,  $Z = 4$ ,  $\lambda(\text{Mo-K}\alpha) = 0.71073$  Å, 78414 reflections, 33033 unique ( $R_{\text{int}} = 0.087$ ),  $R_1 = 0.0582$  for  $I > 2\sigma(I)$ ,  $wR_2 = 0.1254$ . CCDC 247397–247400. See <http://www.rsc.org/suppdata/cc/b4/b412152j/> for crystallographic data in .cif or other electronic format.

§ A difference of 196 mV corresponds to 4.5 kcal mol<sup>−1</sup> in total free energy. Considering the usual experimental uncertainties and the approximations used to compute free energies in solution, the agreement between theory and experiment is remarkable.

¶ Owing to systematic error cancellations, we expect the potential differences ( $\Delta E$ ) to be more accurate than the actual potentials.

- E. I. Solomon, D. W. Randall and T. Glaser, *Coord. Chem. Rev.*, 2000, **200–202**, 595–632.
- Y. Lu, in *Comprehensive Coordination Chemistry II*, eds. L. Que, Jr. and W. B. Tolman, Elsevier, Oxford, UK, 2003, vol. 8, pp. 91–122 and references cited therein.
- (a) C. Harding, V. McKee and J. Nelson, *J. Am. Chem. Soc.*, 1991, **113**, 9684–9685; (b) M. E. Barr, P. H. Smith, W. E. Antholine and B. Spencer, *J. Chem. Soc., Chem. Commun.*, 1993, 1649–1652; (c) C. Harding, J. Nelson, M. C. R. Symons and J. Wyatt, *J. Chem. Soc., Chem. Commun.*, 1994, 2499–2500; (d) R. P. Houser, V. G. Young, Jr. and W. B. Tolman, *J. Am. Chem. Soc.*, 1996, **118**, 2101–2102; (e) C. He and S. J. Lippard, *Inorg. Chem.*, 2000, **39**, 5225–5231; (f) R. Gupta, Z. H. Zhang, D. Powell, M. P. Hendrich and A. S. Borovik, *Inorg. Chem.*, 2002, **41**, 5100–5106.
- (a) D. D. LeCloux, R. Davydov and S. J. Lippard, *J. Am. Chem. Soc.*, 1998, **120**, 6810–6811; (b) J. R. Hagadorn, T. I. Zahn, L. Que, Jr. and W. B. Tolman, *Dalton Trans.*, 2003, 1790–1794.
- S. B. Harkins and J. C. Peters, *J. Am. Chem. Soc.*, 2004, **126**, 2885–2893.
- (a) M. G. B. Drew, D. A. Edwards and R. Richards, *J. Chem. Soc., Dalton Trans.*, 1977, 299–303; (b) P. F. Rodesiler and E. L. Amma, *J. Chem. Soc., Chem. Commun.*, 1974, 599–600.
- (a) F. E. Brinckman, H. S. Haiss and R. A. Robb, *Inorg. Chem.*, 1965, **4**, 936–942; (b) J. E. O'Connor, G. A. Janusonis and E. R. Corey, *Chem. Commun.*, 1968, 445–446.
- (a) J. Barker and M. Kilner, *Coord. Chem. Rev.*, 1994, **133**, 219–300; (b) F. T. Edelmann, D. M. M. Freckmann and H. Schumann, *Chem. Rev.*, 2002, **102**, 1851–1896 and references cited therein.
- (a) S. Maier, W. Hiller, J. Strähle, C. Ergezinger and K. Dehnicke, *Z. Naturforsch., Teil B*, 1988, **43**, 1628–1632; (b) F. A. Cotton, X. Feng, M. Matusz and R. Poli, *J. Am. Chem. Soc.*, 1988, **110**, 7077–7083; (c) B. S. Lim, A. Rahtu, J.-S. Park and R. G. Gordon, *Inorg. Chem.*, 2003, **42**, 7951–7958.
- All potentials referenced to  $\text{Fc}/\text{Fc}^+$ .
- (a) M.-H. Baik and R. A. Friesner, *J. Phys. Chem. A*, 2002, **106**, 7407–7412; (b) M.-H. Baik, C. K. Schauer and T. Ziegler, *J. Am. Chem. Soc.*, 2002, **124**, 11167–11181; (c) M.-H. Baik, J. S. Silverman, I. V. Yang, P. A. Ropp, V. A. Szalai, W. Yang and H. H. Thorp, *J. Phys. Chem. B*, 2001, **105**, 6437–6444.
- R. R. Gagné, C. A. Koval, T. J. Smith and M. C. Cimolino, *J. Am. Chem. Soc.*, 1979, **101**, 4571–4580.
- I. Mayer, *Int. J. Quantum Chem.*, 1986, **29**, 477–483.
- A computed M–M bond order that is lower than 0.3 indicates that there is no bond present. For an example of a dimer with a typical M–M bond that changes notably as a function of the oxidation state, see: M.-H. Baik, R. A. Friesner and G. Parkin, *Polyhedron*, 2004, **23**, 2879–2900.